

SATELLITE ALIGNMENT: I. DISTRIBUTION OF SUBSTRUCTURES AND THEIR DEPENDENCE ON ASSEMBLY HISTORY FROM N-BODY SIMULATIONS

YANG OCEAN WANG^{1,4}, W. P. LIN^{1,4,5}, X. KANG², AARON DUTTON³, YU YU^{1,4} & ANDREA.V. MACCIÒ³

Draft version December 3, 2024

ABSTRACT

Observations have shown that the spatial distribution of satellite galaxies is not random, but aligned with the major axes of central galaxies. This alignment is dependent on galaxy properties, such that red satellites are more strongly aligned than blue satellites. Theoretical work done to interpret this phenomena has found that it is due to the non-spherical nature of dark matter halos. However, most studies over-predict the alignment signal under the assumption that the central galaxy shape follows the shape of the host halo. It is also not clear whether the color dependence of alignment is due to an assembly bias or an evolution effect. In this paper we study these problems using a cosmological N-body simulation. Subhalos are used to trace the positions of satellite galaxies. It is found that the shape of dark matter halos are mis-aligned at different radii. If the central galaxy shares the same shape as the inner host halo, then the alignment effect is weaker and agrees with observational data. However, it predicts almost no dependence of alignment on the color of satellite galaxies, though the late accreted subhalos show stronger alignment with the outer layer of the host halo than their early accreted counterparts. We find that this is due to the limitation of pure N-body simulations that satellite galaxies without associated subhalos (‘orphan galaxies’) are not resolved. These orphan (mostly red) satellites often reside in the inner region of host halos and should follow the shape of the host halo in the inner region.

Subject headings: methods: N-body simulations – methods: statistical – galaxies:halos – galaxies: structure – dark matter: distribution: assembly

1. INTRODUCTION

In the currently favored cold dark matter cosmology, cosmic structures are built up of dark matter haloes. The formation of haloes is hierarchical, in that small haloes form first and subsequently merge to form bigger ones. After the mergers, smaller haloes become the subhalos of the more massive host halo. Galaxies are thought to form in the center of haloes (White & Rees 1978), and most of them become satellites when their host haloes merge with a more massive one. After the mergers, the motions of subhalos/satellites are mainly dominated by the gravitational potential of the host, and in principle they can be well traced using numerical simulations (e.g., Springel et al. 2001) or analytical models (e.g., Taylor & Babul 2001; Gan et al. 2010).

It was found from N-body simulations (e.g., Jing & Suto 2002) that dark matter haloes are not spherical, but rather they are tri-axial. The non-spherical shapes are related to the formation history of haloes, which happen preferentially along filaments. As the assembly history of a halo should be imprinted in the phase-space distribution of its satellite galaxies, observational attempts have been made to infer halo

shapes using satellite distributions. Though the task is challenging, progress has been made using the distribution of stellar velocity (Olling & Merrifield 2000), satellite tidal streams (Ibata et al. 2001; Lux et al. 2012; Vera-Ciro & Helmi 2013), and gravitational lensing (e.g., Hoekstra et al. 2004; Er & Schneider 2011).

The measurements of halo shapes from satellite kinematics or weak lensing rely on an estimate of the host potential. In fact, more useful insight can also be gained from the pure spatial distribution of satellites. Most studies have focused on how satellites distribute with respect to the shape of the central galaxy, named as galaxy alignment. The observational study of the alignment of galaxies has a long history (e.g., Holmberg 1969; Brainerd 2005; Yang et al. 2006; Azzaro et al. 2007; Libeskind et al. 2007). Based on large galaxy surveys such as 2dFGRS and SDSS, there is general agreement that the distribution of satellite galaxies is preferred along the major axis of the central galaxy. Moreover the alignment signal depends on galaxy color. Yang et al. (2006) found a stronger alignment signal for red central galaxies or red satellites. Such an effect is also seen at high redshift (Wang et al. 2010).

A rough idea to explain the observed galaxy alignment is that if satellite galaxies follow the distribution of dark matter, and the central galaxy also shares a similar shape as the host halo, then the non-spherical nature of dark matter halos naturally produces an alignment effect. In fact, many theoretical works follow this idea (Lee, Kang & Jing 2005; Agustsson & Brainerd 2006; Kang et al. 2005, 2007; Libeskind et al. 2007; Faltenbacher et al. 2007;

wangyang,linwp@shao.ac.cn

¹ Key Laboratory for Research in Galaxies and Cosmology, Shanghai Astronomical Observatory, Chinese Academy of Science, 80 Nandan Road, Shanghai 200030, China

² The Partner Group of MPI for Astronomy, Purple Mountain Observatory, 2 West Beijing Road, Nanjing 210008, China

³ Max-Planck-Institute für Astronomie, Königstuhl 17, 69117, Heidelberg, Germany

⁴ Graduate School, University of the Chinese Academy of Sciences, 19A, Yuquan Road, Beijing, China

⁵ Center for Astronomy and Astrophysics, Shanghai Jiaotong University, Shanghai 200240, China

Bailin et al. 2008; Faltenbacher et al. 2008, 2009; Agustsson & Brainerd 2010; Deason et al. 2011). However, most studies over-predict the alignment signal when the central galaxy is assumed to follow the same shape as the whole host halo. Furthermore, most studies are unable to reproduce the alignment dependence on galaxy color unless a dependence of central galaxy alignment with the host halo is assumed (Agustsson & Brainerd 2010).

The main difficulty faced by theoretical studies of galaxy alignment is how to assign the shape of the central galaxy. The most natural way is to use hydro-simulations including physics governing galaxy formation, such as gas cooling, star formation and feedback. Unfortunately, current simulations are typically unable to produce a galaxy population which matches observational data (see however Vogelsberger et al. 2013 and references therein). In this paper, we revisit the problem of galaxy alignment using an N-body simulation which allows good statistics with a large number of massive halos. Since the simulation does not include models for galaxy formation, we instead use the subhalos as tracers of satellite galaxies. For central galaxies, we follow previous studies and assume that the shape of the central galaxy follows the shape of its host halo. In our study, the halo shape is measured at different iso-density surfaces using a method different from previous studies. In an upcoming paper, we will present the results using SPH simulations performed with Gadget-2 (paper II, in preparation).

In addition to the overall alignment signal, we investigate the dependence of alignment on the accretion and formation history of subhalos. Since red satellites have stronger alignment with central galaxies (e.g, Yang et al. 2006), and in general red satellites are accreted at earlier times, it is natural to ask whether the stronger alignment of red satellites is already set before their accretion into the host halo or it is an evolution effect that red satellites follow more closely the shape of dark matter halo after accretion. To study this question, we study the alignment of subhalos as a function of their formation and accretion time. To probe if the color dependence is imprinted in the large-scale environment or is due to an evolution effect, we also study the alignment of neighboring haloes which are within one to a few virial radii from the host haloes.

The paper is organized as follows. In section 2, we briefly describe the simulation and how we determine the shapes of dark matter halos. In section 3 and 4, we show the alignment of subhalos and its dependence on the subhalo mass. In section 5 we investigate if the alignment signal is dependent on the accretion or formation time of the subhalo, and present the results of alignment of neighboring haloes. We summarize and briefly discuss our results in section 6.

2. THE SIMULATION AND TRI-AXIAL HALO SHAPE

The cosmological simulation used in this paper was performed using the massive parallel code Gadget-2 (Springel et al. 2001; Springel 2005) and evolved from redshift $z = 120$ to the present epoch in a cubic box of 100Mpc/h with 512^3 dark matter particles, assuming a flat Λ CDM ‘‘concordance’’ cosmology with $\Omega_m = 0.268$, $\Omega_\Lambda = 0.732$, $\sigma_8 = 0.85$. A Plummer softening length of 4.5kpc was adopted and each dark matter particle

has a mass of about $5.5 \times 10^8 h^{-1} M_\odot$. The simulation has been widely used in previous studies (e.g., Jing et al. 2006; Zhu et al. 2006; Lin et al. 2006) and the readers are referred to these papers for more details of the simulation. In total 62 snapshots between $z = 15$ and $z = 0$ have been used to construct the merger history of halos and subhalos. All halos were found using the standard friends-of-friends algorithm with a linking length of 0.2 times the mean particle separation, while subhalos were found using the SUBFIND routine (Springel et al. 2001b).

We select host halos as those with a mass larger than $10^{12} M_\odot$ (to mimic the data of Yang et al. 2006). In our simulation there are about 2000 host halos in total, at redshift $z = 0$. Then we re-select host halos with θ_{err} of inner axes less than 5° . Here θ_{err} is the error on determining the axis given by following equation

$$\theta_{\text{err}} = \frac{1}{2\sqrt{N}} \frac{\sqrt{r}}{1-r}, \quad (1)$$

where N is the number of particles used and r is the relevant axis ratio: b/a for the major axis, c/b for the minor axis, and $\max(b/a, c/b)$ for the intermediate axis (here a, b, c are the lengths of the axes with $a \geq b \geq c$) (c.f. Bailin & Steinmetz 2004). There are 1604 haloes that survive our two cuts. In Table. 1 we list the number of host halos in different mass bins. Unless otherwise specified, the following analysis will use the same halo catalogue as described in Table. 1.

There are various methods to determine the shape of halos and they differ in details (Bailin & Steinmetz 2005). In the most widely used method, the axes of a dark matter halo are calculated by its overall inertia tensor defined as

$$I_{ij} = \sum_n x_{i,n} x_{j,n}, \quad (2)$$

where $x_{i,n}$ is the distance of particle n from the halo center in dimension i and the summation is over all particles in a halo. In the 3D configuration space $i, j = 1, 2, 3$. The three eigenvectors of I_{ij} define the orientation of the three axes of a halo, and the eigenvalues are related to the rms along the corresponding eigenvectors. The halo shape determined in this way should be closely correlated with the large scale environment of the halo, for example, external tidal field or large nearby filaments (Porciani et al. 2002).

An improved version of the above method uses the reduced inertia tensor defined as

$$I_{ij} = \sum_n \frac{x_{i,n} x_{j,n}}{r_n^2}, \quad (3)$$

which can alleviate the contamination of substructures (Gerhard 1983; Bailin & Steinmetz 2005). Here r_n is the distance of the n th particle from the halo center. In this work, when we calculate the axes for the whole halo, we use this reduced inertia tensor.

Since dark matter halos form hierarchically, the inertia tensors of the whole halo might not precisely describe its internal orientation or that of the central galaxy residing in it. Therefore, following Jing & Suto (2002) we use different iso-density surfaces to determine the axes of a halo. The local density at a particle position is calculated by using the smoothed-particle-hydrodynamics

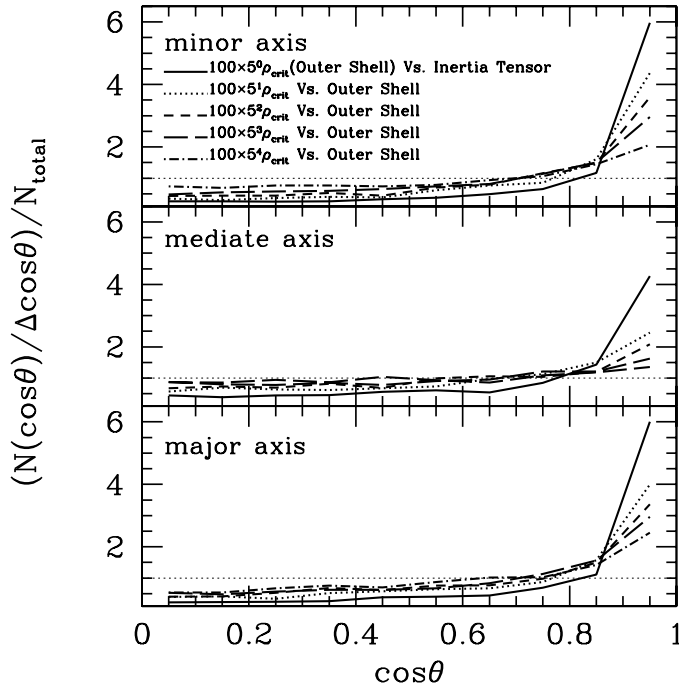


Figure 1. Comparison of the angle between the axes determined from two different methods (iso-density and reduced inertia tensor). The top, middle and bottom panels are for the minor, mediate, and major axes, respectively. The solid lines show the angle between the axes of the outer shell (from the iso-density method) and that determined from the inertia tensor. Other lines are the alignment between the different shells using the iso-density method.

(SPH) method. We select those particles with local density within a narrow bin as an input list for the group finder and apply the FoF method again to find subhalos using a smaller linking length. To exclude particles from subhalos and eliminate their influence on the shape determination of the host halo, only those particles within the largest sub-group are retained. Finally the iso-density surfaces of a halo are built up and then the axes of them can be calculated by fitting with a tri-axial ellipsoid.

Following Jing & Suto (2002), we determine the axes for five different iso-density surfaces, for which the n^{th} bin has local density of $100 \times 5^{n-1}$ ($n = 1, 2, 3, 4, 5$) times the cosmic critical density. The mean radius of each elliptical surface is approximately 0.6, 0.4, 0.25, 0.12, 0.06 of the virial radius respectively. The orientation of the five iso-density surfaces represents the orientation of different parts of a halo, from the most inner part to the outer part. For convenience, in the following content we will call the axis of the most outer part of the halo as “*outer axis*” ($n=1$), the axis of the most inner part of the halo as “*inner axis*” ($n=5$) and the axis of intermediate part as “*intermediate axis*” ($n=3$).

Intuitively, the shape of the outer iso-density ellipsoids should be closely correlated to that of the whole halo. In Fig. 1 we plot the alignment between the axes of the iso-density ellipsoid and that of the halo inertia tensor. It is not surprising to find that the outer axes align strongly with the axes derived from the inertia tensor of the whole halo, and that the strength of alignment for the inner axes becomes weaker (but still significant). Interestingly but nothing unusual, it commendably demonstrates again the hierarchical structure of dark matter halos. The results also show that

there is non-negligible mis-alignment between halo major “*inner axis*” and major “*outer axis*”, which may imply the mild alignment signal between BCG orientation and satellite distribution, as presented in the next section. The alignment between the ‘inner’ and ‘outer’ axes is stronger with increasing halo mass, with average alignment angles of 46.2° , 38.8° , 26.0° , for host halos with $10^{12}M_\odot < M_{\text{vir}} < 10^{13}M_\odot$, $10^{13}M_\odot < M_{\text{vir}} < 10^{14}M_\odot$ and $M_{\text{vir}} \geq 10^{14}M_\odot$, respectively. Although determining axes will suffer from the limited number of particles especially for small halos, our strategy which excludes host halos with less accuracy ($\theta_{\text{err}} > 5^\circ$) can alleviate this problem and making the above results more reliable.

3. SPATIAL DISTRIBUTION OF SUBHALOS AND NEIGHBORING HALOS

In this section, we present the spatial distribution of subhalos and the neighboring halos from our simulation. For each host halo, we place a central galaxy at its center whose shape is set to follow the shape of the host dark matter halo (either inner, intermediate or outer axis). The neighboring halos are defined as individual halos which are less massive than the host halo and reside within the range of $1 - 3r_{\text{vir}}$ from the center of host halo. To obtain more robust results, we limit subhalos to be more massive than $1.65 \times 10^{10}h^{-1}M_\odot$ (containing more than 30 particles) and neighboring halos more massive than $5.5 \times 10^{10}h^{-1}M_\odot$ (containing more than 100 particles). Table. 1 lists the number of subhalos and neighboring halos in each mass bin.

Table 1
Number of host halos in different mass bins, and subhalos and neighboring halos with different masses of their host or of themselves.

Range of $M_{\text{host}}/[h^{-1}M_\odot]$ ^a	$10^{12} \sim 10^{13}$	$10^{13} \sim 10^{14}$	$\geq 10^{14}$
Host Halo	1206	374	24
Subhalo	4193	7175	3793
Neighboring Halo	1703	3238	1625
Range of $M_{\text{self}}/[h^{-1}M_\odot]$ ^b	$10^{10} \sim 10^{11}$	$10^{11} \sim 10^{12}$	$\geq 10^{12}$
Subhalo	11609	3178	374
Neighboring Halo	2961	3249	356

^a Host halos with their inner axes less accurate than 5° and their subhalos and neighboring halos are excluded from this table.

^b Note that we set a minimum number of 30 and 100 particles for subhalos and neighboring halos, so $10^{10} \sim 10^{11}h^{-1}M_\odot$ means about $1.65 \times 10^{10} \sim 10^{11}h^{-1}M_\odot$ for subhalos and $5.5 \times 10^{10} \sim 10^{11}h^{-1}M_\odot$ for neighboring halos.

The alignment signal is described as the distribution of angular separation between the axis of the host halo and the connecting line between the centers of the host halo and each subhalo/neighboring halo. The distribution is described as,

$$P(\theta) = \frac{N(\theta)}{\langle N_R(\theta) \rangle}, \quad (4)$$

where $N(\theta)$ is the counts of subhalos (or neighboring halos) in bin θ , while $\langle N_R(\theta) \rangle$ is the average counts of random samples in the same bin. So $P(\theta) = 1$ means the absence of any alignment, while $P(\theta) > 1$ at small θ implies a distribution with a preferred alignment along the major axis.

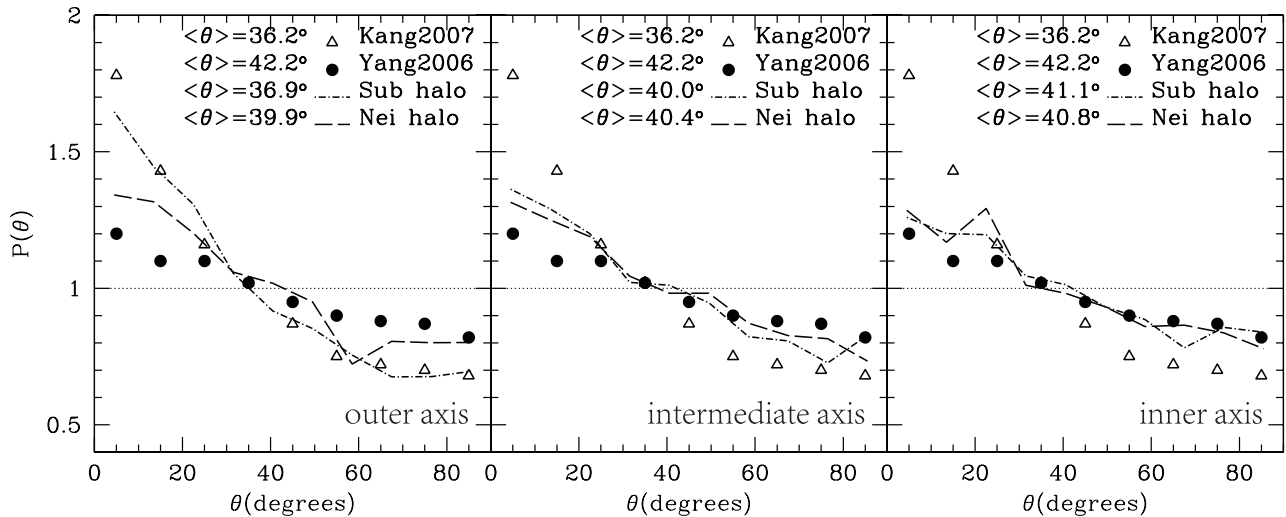


Figure 2. The angular distribution of sub-halos and neighboring halos along the major axis of host halo, converted to the compatible format as Yang and Kang’s work. The short and long dashed lines represent the sub-halos and neighboring halos respectively. The open triangles are theoretical results of Kang et al. (2007) while the solid dots are the observations of Yang et al. (2006). From the left to the right panels, the lines represent statistical results using the major axis of the most outer part, intermediate part and most inner part of halos, respectively. The horizontal dot line means a random distribution. For convenience, the legend “neighboring” is replaced with “Nei” here and in all plots throughout.

To compare with the observational results of Yang et al. (2006), here we do the analysis in 2D space. We first calculate the axes in 3D space, and then project them onto the X-Y plane. The angular position is then obtained for every subhalo/neighbouring halo using its projected position in the same plane. To generate the random sample, for each host halo containing N subhalos, we produce N subhalos in 3D space with a spherical random distribution. In principle, the produced random sample should share the same radial distribution of the real subhalos in each host halo. However, as our calculation is only dependent on the angular separation, our results are not affected by this requirement.

In Fig. 2 we show the alignment along the major axes of central galaxies. The left, middle and right panels show the results assuming that the central galaxies follow the shape of their host halos defined at the outer, intermediate and inner axes. In each panel the dotted and dashed lines are for subhalos and neighboring halos, respectively. For comparison with other results, we also plot the observational work of Yang et al. (2006), and the theoretical one by Kang et al. (2007) as circles and triangles in each panel.

Fig. 2 shows that both subhalos and neighboring halos are aligned with the major axes of central galaxies. The signal is stronger than the data (solid points) if the central galaxy follows the shape of the dark matter halo at the outer or intermediate axes (left and middle panels). Our results are consistent with those of Kang et al. (2007), who used satellite galaxies from their SAMs and have found strong alignment if central galaxy follows the shape of the whole dark matter halo. Kang et al. (2007) pointed out that some observational effects, such as the flux-limit, redshift-space distortions and the galaxy group finder, could cause a shallowing of the alignment signal, but these would not be enough to reconcile the simulations with observations. They further proposed that the observed alignment signal could be reproduced if the spin of the central galaxy aligns with that of dark matter halo.

Our result shows that there may be another way to remove such a discrepancy with observations. As showed in the right panel of Fig. 2, the predicted alignment signal is close to the data if the shape of the central galaxy follows the shape defined at the inner halo region. This is also consistent with the results of Faltenbacher et al. (2009) in which they also found only a weak misalignment if using the inner halo to define the shape of central galaxy, although they use a different method to measure the halo shape.

It is also found from Fig. 2 that the alignment of neighboring halos is similar to that of the subhalos. There seems to be a slight evolution effect that subhalos’ alignment is stronger if the central galaxy follows the outer shape of dark matter halo (left panel). However, the predicted alignment signal is too strong in this case, thus it can not account for the observed color dependence of satellite alignment. If the central galaxy follows the shape of the inner axis, and blue satellite galaxies are recently accreted from neighboring halos, then their alignment should be identical to that of the red satellites (subhalos in our case). To explain the observed color dependence, it will require that either blue (red) satellites are not random sample of neighboring halos (subhalos). We will later investigate if the color dependence arises from the assembly bias of satellite galaxies.

The right panel of Fig. 2 shows that if the central galaxy follows the inner shape of the dark matter halo, then the predicted alignment signal is more or less consistent with the data. However, it is not implied that this is the only way to reproduce the observed alignment signal. It indicates that some degree of misalignment between the central galaxy and the overall shape of dark matter halo has to be assumed. For example, Kang et al. (2007) and Agustsson & Brainerd (2010) both have found that if the minor axis of central galaxies follows the angular momentum of the dark matter halo, then the alignment of satellites is also closer to the observational data.

The observed alignment effect can also be reproduced if the central galaxy follows the overall shape of the dark

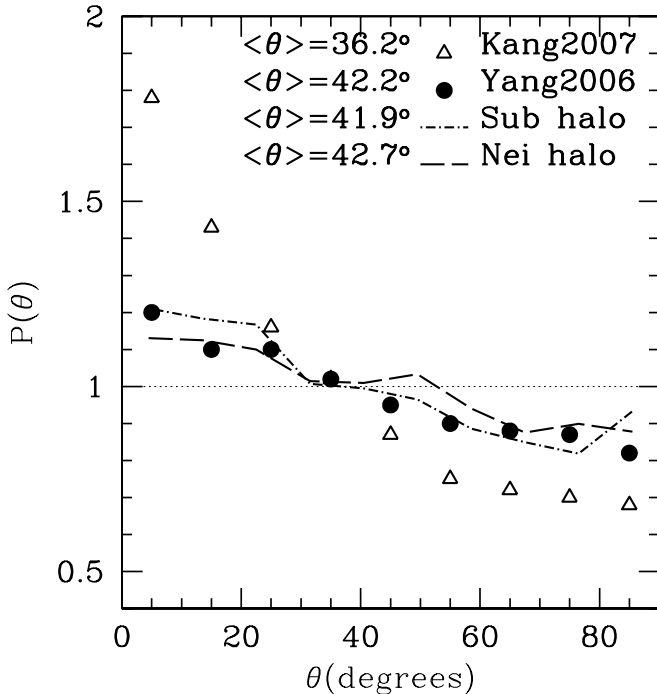


Figure 3. The angular distribution of sub-halos and neighboring halos along a designed axis of center galaxy. See the main text for more details.

matter halo, but with some distribution. Fig. 3 shows the results when the angle between the major axes of the central galaxy and the host halo follows a Gaussian distribution with a mean of 0° and a standard deviation of 25° . It is seen that the observed alignment signal is well reproduced. Some previous works find results consistent with this: Bailin & Steinmetz (2005) found a misalignment between the angular momentum vector and the minor axis, with a mean value of about 25° ; Bett et al. (2010) found that there is a median angle of 25° between the angular momentum vectors of inner ($\leq 0.25R_{\text{vir}}$) part and the whole halo. In fact, there is observational evidence for a mis-alignment angle of about 23° between the major axis of brightest central galaxies (BCG) and that of their dark matter halos inferred from the distribution of satellite galaxies (Wang et al. 2008). In addition, a larger mis-alignment angle of about 35° was also suggested from gravitational shear-intrinsic ellipticity correlation of luminous red galaxies (Okumura & Jing 2009; Okumura et al. 2009).

So far, there is no definitive way to assign a shape to the central galaxy. The most promising way should be the one which can reproduce not only the overall alignment of satellites, but their dependence on galaxy properties. Studies based on N-body simulations and semi-analytical models for galaxy formation (Kang et al. 2007; Agustsson & Brainerd 2010; Libeskind et al. 2005; Zentner et al. 2005) have made some progress to achieve this goal. However, these studies still face problems. First, the predicted total alignment signal is still stronger than observations. Second, the color dependence of satellites in the models themselves are not correctly reproduced (however, see Agustsson & Brainerd 2010). Third, it is difficult to interpret the contamination of interlopers in observations.

In our simulations we have no galaxies, only subhalos.

Thus we are unable to explore the dependence of alignment on galaxy properties. However, as galaxy properties are closely related to the halo (subhalo) mass and accretion time (Yang et al. 2012), we could learn the shape of the central galaxy from the dependence of alignment on the mass of host halos and subhalos. In particular, we want to study if the alignment is dependent on the accretion/formation time of subhalos and will present such results in the following sections.

4. DEPENDENCE ON HALO/SUBHALO MASS

Observationally, it was found that the alignment of satellites is stronger in massive halos, and it is even stronger for red satellites in massive red central galaxies (c.f., Yang et al. 2006). Such a mass dependence should be imprinted in the alignment of subhalos/neighboring halos. In this section, we investigate the dependence of alignment on the host halo mass and the mass of subhalos/neighboring halos themselves. Different from the previous section, here we give the results in 3D space since it gives a stronger alignment signal in real space. Fig. 4 shows the effects of host halo mass on the alignment of subhalos and neighboring halos. Note that the error-bars are for the 1σ standard deviation of the mean throughout the paper. It is found that more massive host halos have a stronger alignment signal. Though subhalos/neighboring halos preferentially align along the “outer axis”, it seems that dependence on halo mass is stronger for the alignment along the “inner axis”. This reflects the dependence of central-to-outer alignment strength with halo mass. Given the fact that more massive BCGs have redder colors, the results for “inner axis” are in agreement with observational results of stronger alignment for red central galaxies than blue central galaxies (Yang et al. 2006), as well as the results from a semi-analytical model (e.g., Kang et al. 2007).

In Fig. 5 we show the alignment of subhalos/neighboring halos with dependence on their own mass. Contrary to the dependence on the host halo mass, the dependence is quite weak on the mass of subhalos/neighboring halos themselves. Only those most massive subhalos/neighboring halos show a little stronger alignment signal along the “outer axis” of their host halo than less massive ones. We also find that if the mass of subhalos at accretion is used instead, the results are also very similar. Assuming that massive subhalos or neighboring halos harbor redder satellites and the major axis of the central galaxy can be represented by the “inner axis” of host halos, the results of alignment along the “inner axis” (left panels in Fig. 5) can not explain the observational trend that red satellites are better aligned than the blue counterparts (Yang et al. 2006).

Our results above clearly show that the neighboring halos are preferentially distributed along the major outer axes of the host halos. This is easy to understand as the neighboring halos define the local large-scale environment of the host halo which dominate the direction of mass accretion. Also found is that more massive host haloes are stronger aligned with the neighboring halos (lower right panel of Fig. 4) and the most massive neighboring halos have stronger alignment with the host halos (lower right panel of Fig. 5). These results are consistent with the picture that more massive host halos are connected with stronger filaments where more massive

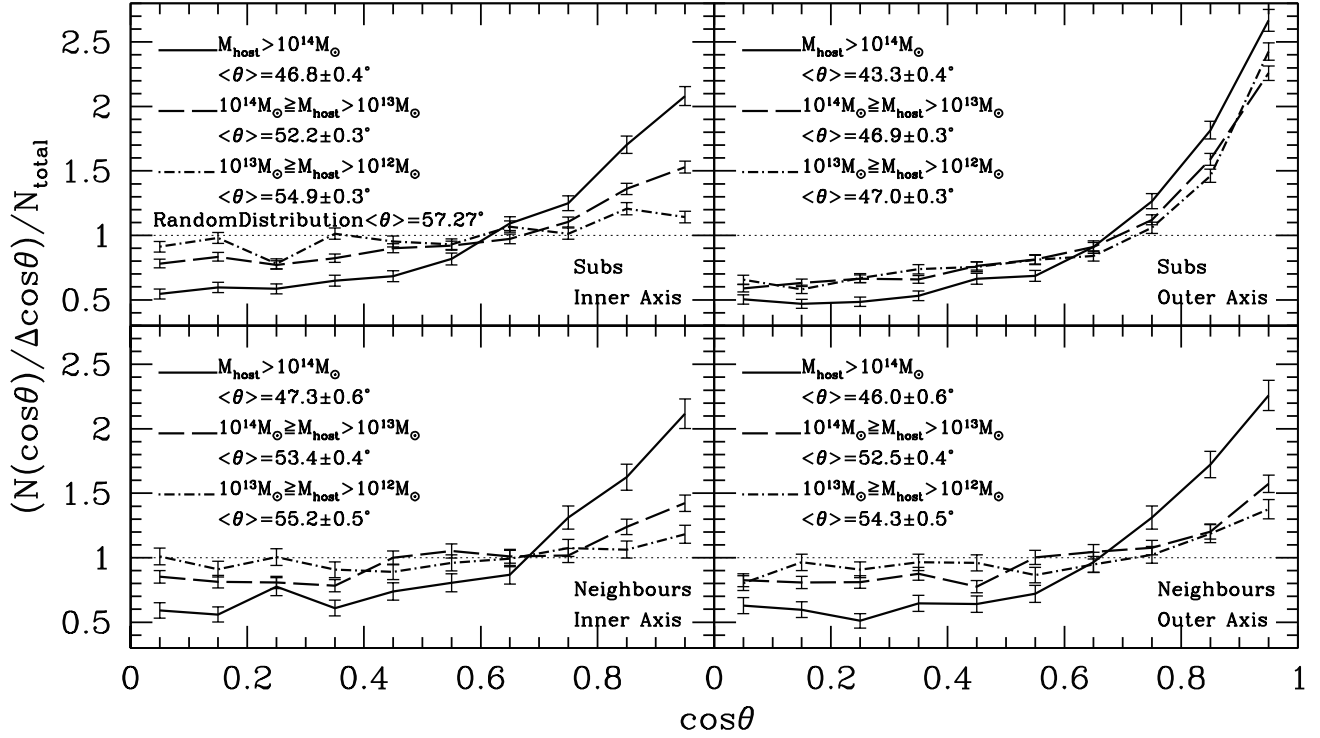


Figure 4. The dependence of the angular distribution for sub-halos (upper panels) or neighboring halos (bottom panels) on host halo mass. The vertical coordinate represents the probability while the horizontal coordinate represents the cosine of the angular separation (see main text for definition). The alignment along “inner axis” and “outer axis” are plotted in the left and right panel respectively. Error bars indicate 1σ standard deviation in each bin. Different lines represent different bins of host halo mass. An isotropic angular distribution corresponds to the horizontal dotted lines.

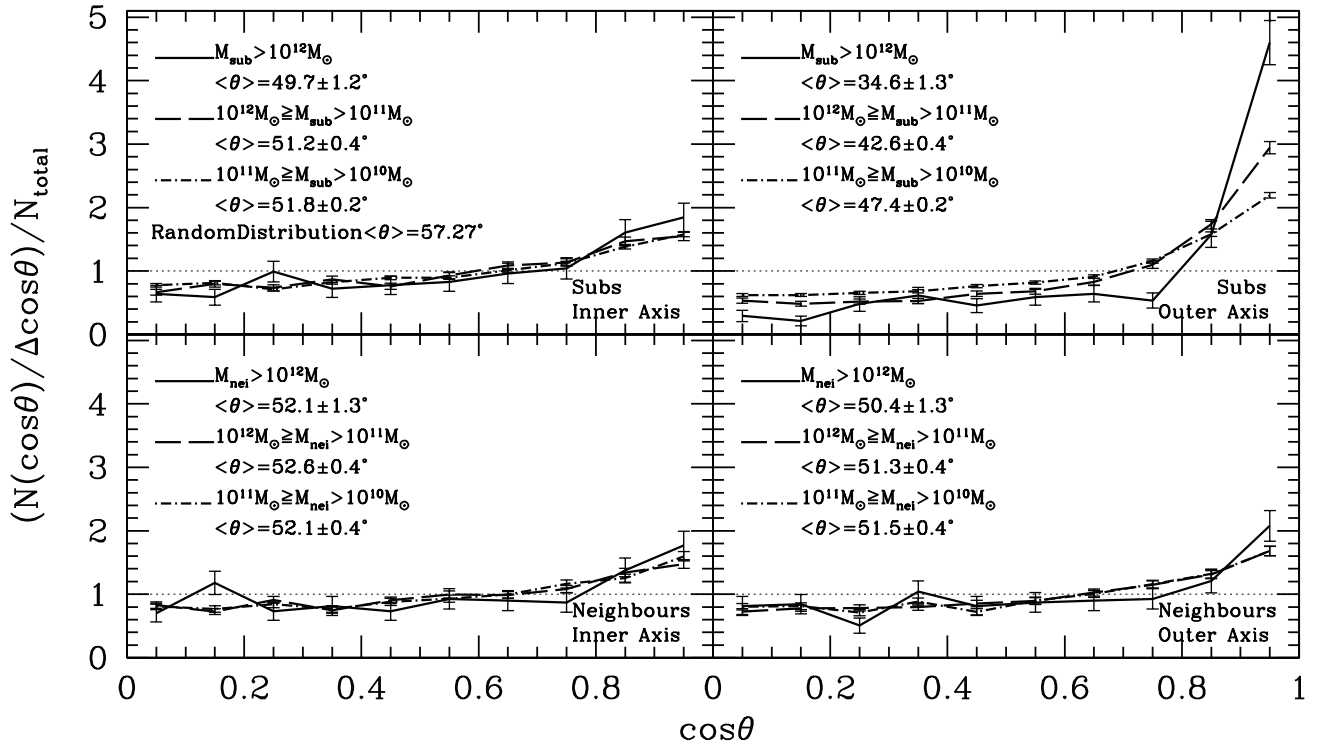


Figure 5. The dependence of angular distribution on the mass of sub-halos or neighboring halos. Other description is the same as Fig. 4 except that different lines are for mass bins of sub-halos/neighboring halos.

subhalos are embedded and accreted along them.

5. DEPENDENCE ON ASSEMBLY HISTORY

Intuitively one would speculate that galaxies which formed earlier (such that their host halos formed earlier) should have a redder color, therefore there could be helpful clues for the dependence of alignment signal on galaxy color from the formation histories of halos. On the other hand, being accreted is an important event for a subhalo. One would expect that subhalos accreted earlier will spend more time within host halos and suffer longer from tidal stripping as well as dynamical friction and thus may lose memory of initial accretion positions, consequently attenuating the alignment signal. However, it is also possible that earlier accreted satellites will experience more gravitational effects from the host, thus following the shape of the host more closely and predicting stronger alignment (Yang et al. 2006). These two effects will compete with each other, and finally determine the alignment of satellite galaxies.

In this section, we focus on the relation between subhalos’ (or neighboring halos’) angular alignment and their assembly history. Here we define two key time points for the formation and evolution of subhalos. A subhalo was once an independent halo before it is accreted into a virialized halo nowadays. We define the time when the progenitor of a subhalo was accreted into a large halo as “*accretion time*”. As subhalos often cross the virial radius of the host halos for a few times (e.g. Ludlow et al. 2009), we use the first time it cross the virial radius as the accretion time. Before being accreted, the progenitor halo evolves as an individual halo, and its mass grows almost monotonically with time (De Lucia et al. 2004). The time when this progenitor halo has assembled half of its mass at the accretion time is defined as its “*formation time*”. For neighboring halos, there is no accretion time to apply since it has not been accreted by the central halo. Therefore we define their “*formation time*” as the time when they accrete half of their mass at $z = 0$ and consider the effect of their “*formation time*” only.

First, we show the distribution of accretion and formation redshifts of all subhalos/neighboring halos in our sample in Fig. 6. The accretion redshifts mostly range from $z = 0$ to $z = 5$. One can find that most subhalos are accreted to their host halos at redshift $z < 1$. This is consistent with previous work De Lucia et al. (2004). Note that here we only analyze the accretion redshifts for those subhalos which finally survive at $z = 0$ in their host halos. In some previous works (e.g., Yang et al. 2011), the statistic of accretion time based on merger trees including un-resolved subhalos are different, which have more accretion events at higher redshift. Also in our simulation there are some subhalos which can not be traced back to their individual halo progenitors due to the resolution of the simulation. Such kind of subhalo accounts for approximately 15% of all subhalos. The formation time distribution of neighboring halos is consistent with the prediction for low mass halos (e.g., Lin et al. 2003).

Fig. 7 shows the angular distribution of subhalos with different accreted redshifts. We choose the 20% of subhalos accreted earliest, the 20% accreted latest and 20% accreted in mid-period from the whole samples and plot their angular distribution along the major axes of their host halos. Note that the use of 20% is arbitrary. We

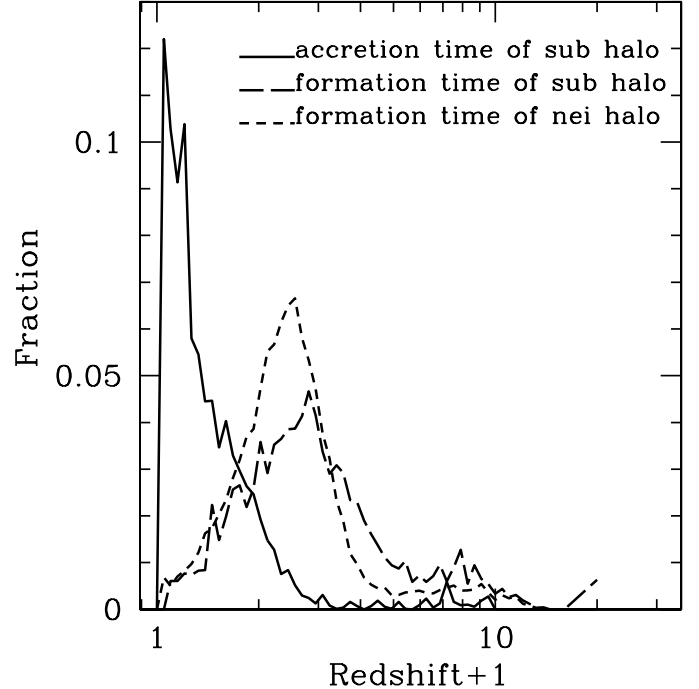


Figure 6. The distribution of formation and accretion redshifts. Solid line represents the distribution of sub-halos’ accretion time, while long and short dashed lines are for the formation time of sub-halos and neighboring halos respectively.

have also tried using choosing criterion of 25%, 33% and 40% (not shown in the plots). As might be expected, it turns out that the difference between early accreted sub-halos and late accreted ones becomes less distinct when the samples include more intermediate accretion redshifts.

The upper panel of Fig. 7 shows that the alignment signals along the inner axes of host halos are almost identical (within the 1σ errors) for the three samples with different formation times. The lower panel shows that later accreted subhalos have significantly stronger alignment with the outer axes of the host halos. From models of galaxy formation (e.g., Kang & van den Bosch 2008; Guo et al. 2011), it is expected that early accreted subhalos should host red satellite galaxies. The observed stronger alignment of red satellites implies that early accreted subhalos should have strong alignment. Indeed such a dependence is seen from the analysis of Agustsson & Brainerd (2010). However, such an expectation is not seen, and is in fact contrary to what we see from Fig. 7 in our work.

To understand this puzzle, we have to note that our results are based on subhalos only, while observations or the analysis of Agustsson & Brainerd (2010) were based on galaxies. To address the dependence of alignment on accretion time of subhalos, we plot the radial distance of subhalos with different accretion time in Fig. 8. The solid line shows that early accreted subhalos stay in the inner host halo, but the late accreted subhalos stay near the virial radius of the host. It is known that subhalos orbiting the inner host halo will suffer from strong tidal forces, and thus are more likely to be disrupted. This effect is more efficient for subhalos with more ‘radial’ orbits, as they have more chance to pass the host center, thus being more exposed to the strong tidal force and

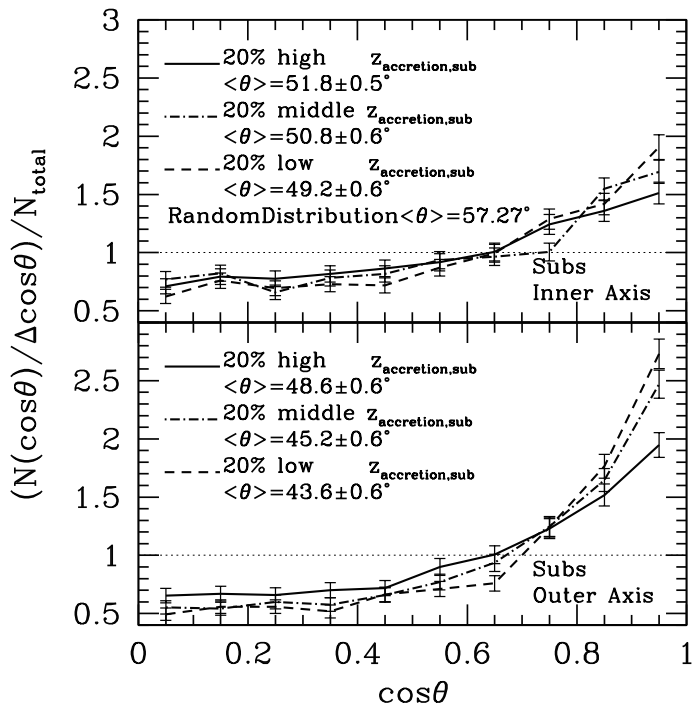


Figure 7. The dependence of angular distribution on accretion redshift. The solid line, dotted dashed line and dashed line are for sub-halos with relatively high, middle and low redshift accretion time respectively. The horizontal dotted line represents an isotropic angular distribution. Error bar indicates 1σ standard deviation in each bin. In each panel, each redshift bin contains 20% of all samples.

being disrupted more efficiently (e.g., Gan et al. 2010). Thus only those with more ‘circular’ orbits will likely survive. Those subhalos with more ‘circular’ orbits will naturally produce a more isotropic distribution. For recently accreted subhalos, the effects of tidal forces are still not strong enough to disrupt them as most of them are still orbiting at the outer host halo.

Although the analysis of Agustsson & Brainerd (2010) made use of an N-body simulation, they do include model galaxies given by the semi-analytical model of Croton et al. (2006). The ‘galaxies’ are traced by subhalos and unresolved subhalos (those disrupted ones). Thus the main difference between Agustsson & Brainerd (2010) and ours is that they include the so-called ‘orphan’ galaxies (Gao et al. 2004) which are not associated with any resolved subhalos, but their positions can be traced using the most-bound particles from the previous resolved subhalos. These orphan galaxies can also be resolved in hydrodynamical simulation with gas physics included as the condensation of baryons boost the density distribution in subhalos, making it more resistant to tidal disruptions (e.g., Macciò et al. 2006).

The ‘orphan’ galaxies are mainly from early accreted subhalos, and most of them are staying in the inner host haloes, contributing significantly to the total galaxy populations (Agustsson & Brainerd 2010). On one hand, these orphan galaxies will include those subhalos with more ‘radial’ orbits, leading to a more aligned distribution. On the other hand, orphan galaxies have orbited in the inner halo for longer time, and they will follow the shape of halo more closely. Under the assumption that central galaxies are also shaped dominantly by the inner

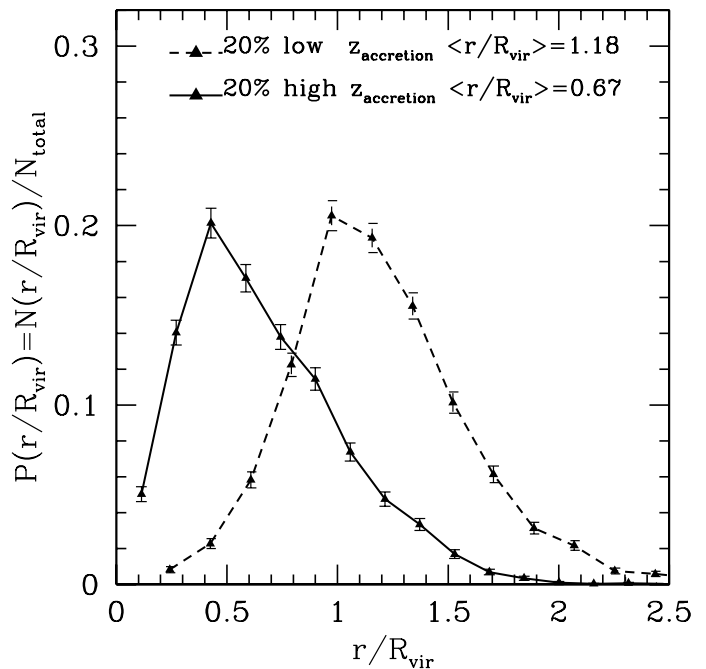


Figure 8. The radial distribution of sub-halos inside host haloes at $z = 0$. The solid line shows the 20% of sub-halos with the earliest (high z) accretion times, while the dashed line shows the 20% of sub-haloes with the latest (low z) accretion times.

host halo, it will predict that red satellites align more strongly with central galaxies than the blue ones which are dominated by recent accreted subhalos at the outer skirts of host haloes. This will be fully consistent with the observations.

Now we investigate the dependence of subhalos’ alignment on their formation time in Fig. 9. Similar to the results shown in Fig. 7 the dependence of alignment of subhalos (upper panels) is identical or slightly stronger in late formed subhalos. This is due to the link between formation and accretion time such that more early formed halos are more likely to be accreted at earlier times. From the lower panel, it is found that for neighboring halos, there is almost no dependence on their formation times.

Therefore, the influence of formation time is similar to that of accretion time. In the bottom panels of Fig. 9, the same method is used as above to explore the influence of formation time on neighboring halos. There is no obvious deviation between two lines in these two panels. The formation time does not influence the distribution of neighboring halos, different from the case for sub-halos. The alignment signal should come from the coherent mass distribution between halos and large scale structures, nothing to do with the formation histories of neighboring halos.

Finally in this section, we show the effects of host halo formation time on the alignment of subhalos/neighboring halos. It is seen from Fig. 10 that the formation time of host halos have weak effects on the alignment of subhalos/neighboring halos. From the Press-Schechter (PS) theory (Press & Schechter 1974), and extended PS theory (Lacey & Cole 1993, 1994; see also Lin et al. 2003), it is known that the formation time of a halo depends on its mass such that more massive halos form on average at later epochs. We should then expect that the alignment of subhalos should be stronger in later-formed

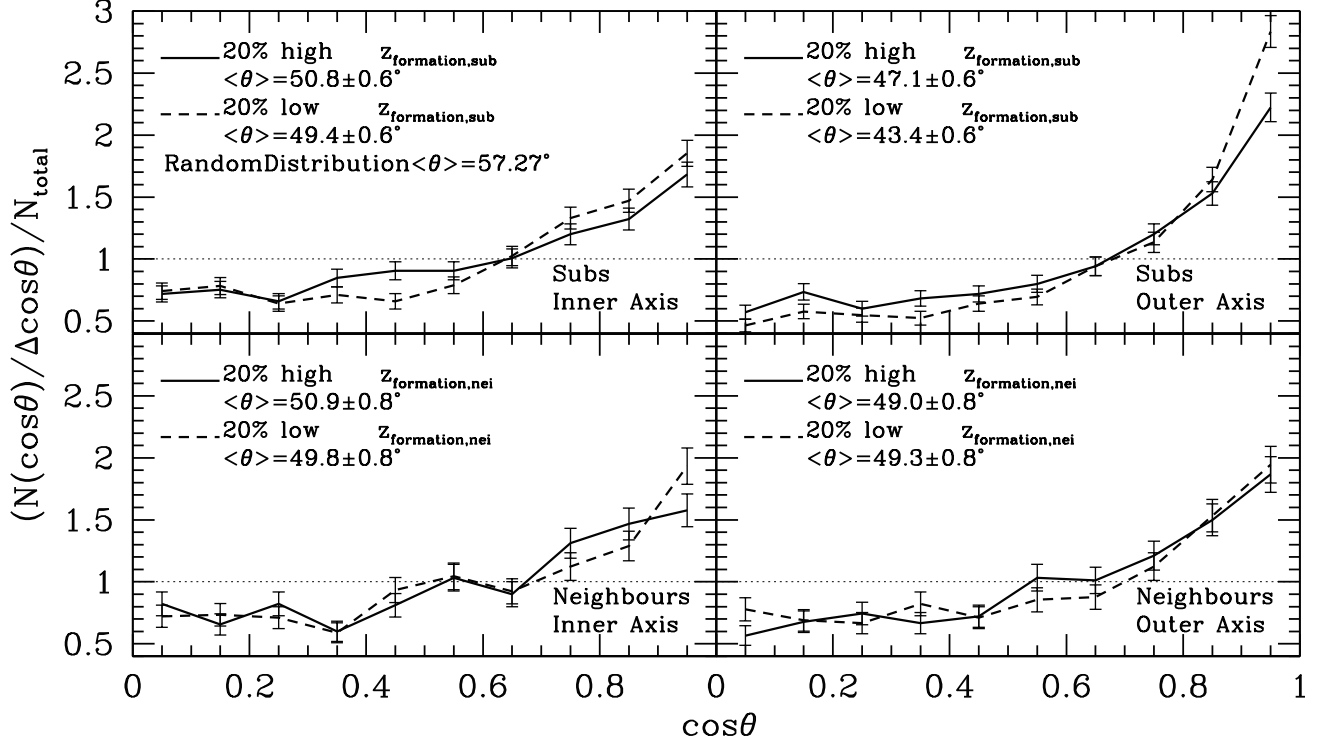


Figure 9. The dependence of angular distribution on formation redshifts for sub-halos (upper panels) and neighboring halos (bottom panels). The alignment along the “inner axis” and “outer axis” are plotted in the left and right panels respectively. The solid line and dashed line are for sub-halos or neighboring halos with relatively high and low formation redshift respectively. The horizontal dotted line represents an isotropic angular distribution. Error bar indicates 1σ standard deviation in each bin.

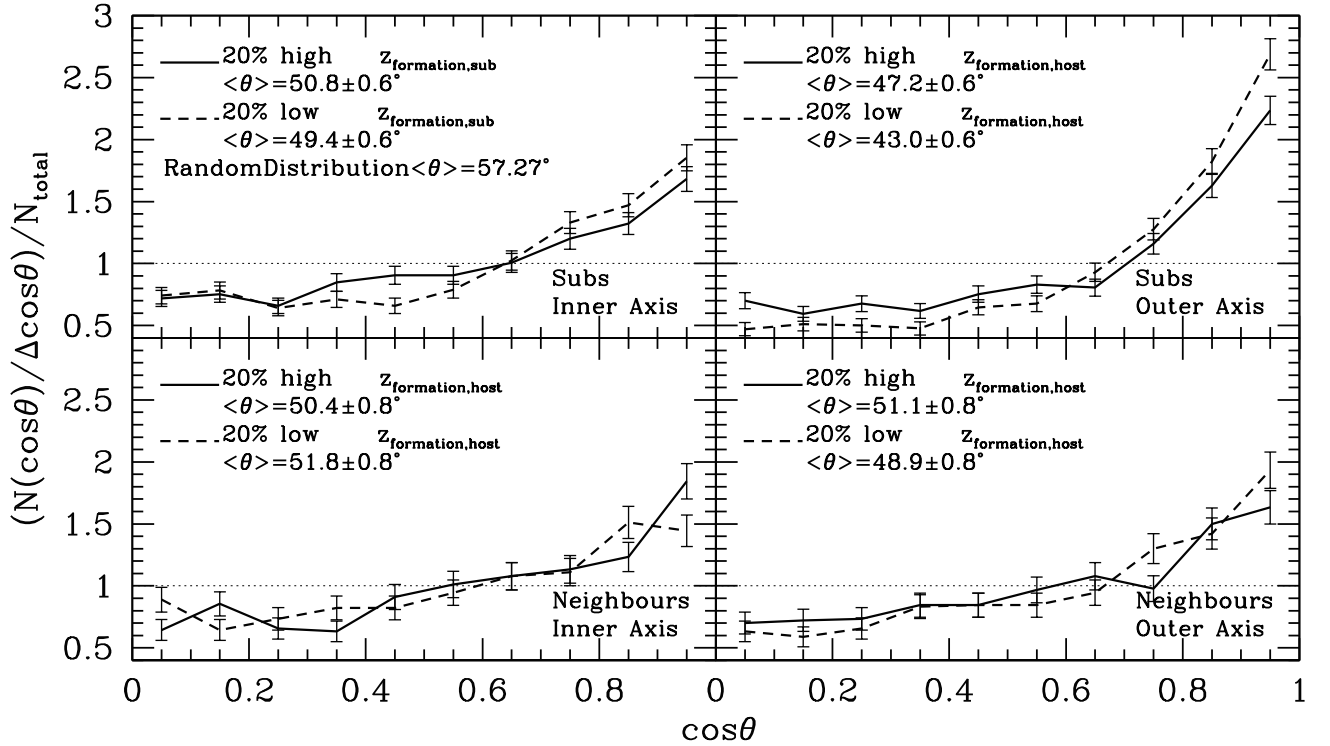


Figure 10. The influence of host halos' formation time on the angular distribution of sub-halos (upper panels) and neighboring halos (bottom panels). The other definition is the same as Fig. 9 except that the bins are divided in the formation time of host halos.

halos, similar to the dependence seen in Fig. 4. However, it should be also noticed that for given halo mass, the formation time has a broad distribution. Thus for a given formation time, there is a wide distribution of halo masses which dilutes the dependence of alignment on halo mass.

6. CONCLUSION & DISCUSSION

Recent observations have found that satellite galaxies are not randomly distributed, but rather they align with the major axis of the central galaxy (e.g., Brainerd 2005; Yang et al. 2006; Azzaro et al. 2007). This intriguing result has generated great interest, with many studies investigating the origin of this phenomenon. The common conclusion from previous studies (e.g., Agustsson & Brainerd 2006; Kang et al. 2007) is that the alignment arises from the non-spherical nature of dark matter halos in the cold dark matter cosmology (e.g., Jing & Suto 2002). However, there is no model which can accurately predict the observed alignment signal and its dependence on galaxy properties. The most difficult part of theoretical modeling is in assigning the shape of central galaxies, and most models do not agree on this aspect.

In this paper, we re-visit the alignment problem using a cosmological N-body simulation. Compared to previous studies, we focus on the origin of the alignment with its dependence on the formation/accretion of subhalos. We investigate if this dependence is from the assembly bias or an evolution effect. Our results are summarized as follows,

- We use a new method to characterize the tri-axial halo shape following Jing & Suto (2002). Unlike the most widely used inertia tensor method which depends on the mass distribution within a given radius and is often contaminated by subhalos, the new method is able to determine the tri-axes of the halo at given local mass over-density, and excludes the effects on subhalos on the shape determination. We find that the measured halo shapes at different radii are well aligned. The mean alignment angle between the inner and outer part of halo is about 26.0° , 38.9° , 48.6° for host halos with $M_{\text{vir}} \geq 10^{14}M_\odot$, $10^{14}M_\odot > M_{\text{vir}} \geq 10^{13}M_\odot$ and $10^{13}M_\odot > M_{\text{vir}} \geq 10^{12}M_\odot$ respectively. The alignment between the inner and outer shapes is increasing with halo mass.
- We study the alignment of both subhalos and neighboring halos around selected host halos. Both subhalos and neighboring haloes are found to align preferentially with the outer axes of host halos. Consistent with previous results (e.g., Kang et al. 2007), we find that the alignment of subhalos is stronger than the data if the outer axis of host halo is used for the shape of central galaxy. Better agreement with the data is achieved if the central galaxy follows the shape of host halo determined at the inner region. We also find that if the alignment between the central galaxy and the outer axis follows a Gaussian distribution with a mean of 0° and a deviation of 25° , the predicted alignment also agree with the data.

- The alignments of subhalos and neighboring halos depend on the mass of the host halos, such that more massive host halos have stronger alignment. This is due to the reasons that more massive halos are more flattened (embedded in filaments) and more massive halos have better alignment between its inner and outer axes. This is consistent with the observations that satellites in massive red central galaxies are more strongly aligned. In Fig 11, we show the dependence of halo flattening on the mass. It is seen that higher mass haloes are more flattened (with lower c/a). Also found is that the inner region of halo is more flattened than the outer part. These results are consistent with previous studies (e.g., Jing & Suto 2002; Allgood et al. 2006; Macciò et al. 2008). We also note that resolution (lower mass halos have fewer particles) has no effect on these results as the distribution shows consistent tendency up to the low-mass end in either case. In Fig 11, we include halos with their axes poorly detected. If these halos are excluded, the line of inner axes goes down at the low mass end. There is weak (if any) dependence of alignment on the mass of subhalos or neighboring halos themselves.

- We study the alignment of subhalos with dependence on their formation time. It is found that there is no dependence along the inner major axes of host halos, and a strong dependence along the outer axes of the host halos such that the early accreted subhalos have lower alignment than the recent accreted ones. This is not consistent with the results of Agustsson & Brainerd (2010), and is also inconsistent with observational evidence that red satellite galaxies (accreted more early) have stronger alignment with the central galaxy than blue satellites.

The main contribution of this paper is that we find that the mis-alignment between the inner and outer axes of the dark matter halos can account for the observed alignment of satellite galaxies including the mass dependence. We confirm the results from most studies that the shape of the central galaxy cannot follow the shape of the whole dark matter halo, otherwise the predicted alignment signal is too strong. However, better agreement with observations can be obtained if the central galaxy follows the shape of the dark matter halo defined at the inner region (measured at an overdensity of $100 \times 5^4 \rho_{\text{crit}}$). In this case, the dependence of alignment on halo mass is also reproduced.

Finally, we discuss whether the stronger alignment of red satellites due to the assembly bias or an evolution effect after accretion. As our simulation do not include models for galaxy formation, we use the subhalo population to address this question. Our conclusion is that the main contribution to the strong alignment of red satellites is from an evolution effect. If red satellites reside in subhalos that form at earlier times or having higher mass at accretion, Fig. 5 and Fig. 9 have shown that those subhalos do not have stronger alignment. Also the alignment of neighboring halos with higher mass or higher formation redshift are also identical. These results indicate

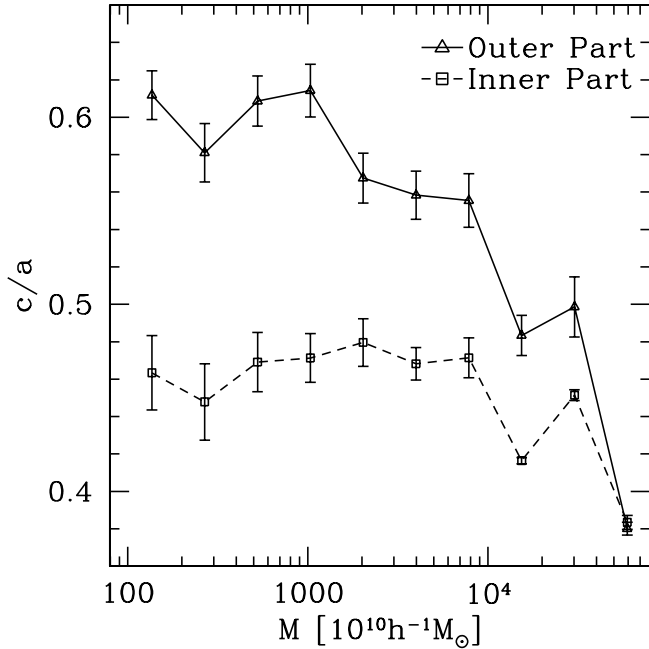


Figure 11. Average axis ratio as a function of halo mass. Every point represent the average c/a for a given mass bin. The error bars stand for 1σ standard deviation. All 2000 halos in our sample are included in this plot.

that the stronger alignment of red satellites is not set at the time of accretion. On the contrary, their strong alignment should come from evolution effects after accretion. Actually, Fig. 2 further shows that the alignment of neighboring halos is lower than the subhalo, implying that subhalos acquire stronger alignment after accretion.

However, our results from Fig. 7 seems not to support the evolution scenario. It shows that early accreted subhalos have lower alignment, indicating a negative evolution effect. It is also inconsistent with the results of Agustsson & Brainerd (2010) who have found that early accreted satellites have stronger alignment. We note that there are differences between our analysis and theirs. In our work, we do not have galaxies, but only subhalos. Also we do not include those disrupted subhalos (‘orphan’ galaxies in the model of Agustsson & Brainerd 2010). Thus in our work, those subhalos accreted at earlier times may have been disrupted, and this effect is more efficient for subhalos with more ‘radial’ orbits as they will come to the host center and suffer strong tidal disruption. In addition, cautions should be taken here that the alignment on ‘inner’ axes are determined less accurately because of limited resolution especially for low-mass halos and also for iso-density surfaces with small ellipticity (the latter one is also the case when determining the major axes observationally). Further investigation using simulations with higher resolution should be helpful.

We simply conclude that to accurately predict the alignment of satellite galaxies found in observations and study its dependence on galaxy properties, we should use hydrodynamical simulation with gas physics and star formation, which can self-consistently predict the shape of central galaxies and the distribution of satellite galaxies around the central galaxy. Although current simulations

with star formation still have difficulties to achieve better agreement with the data, we will show in an upcoming paper that the alignment of satellites and their color dependence can be better reproduced.

We thank the anonymous referee for useful suggestions to improve the manuscript. And we thank Yipeng Jing, Xiaohu Yang, Cheng Li and Jiaxin Han for helpful discussion and comments. WPL acknowledges supports by the NSFC projects (No.10873027, 11121062, 11233005, U1331201). XK is supported by the NSFC (No. 11073055, 11333008), National basic research program of China (2013CB834900) and the Bairen program of the Chinese Academy of Sciences. The work is also supported by the “Strategic Priority Research Program the Emergence of Cosmological Structures” of the Chinese Academy of Sciences Grant No. XDB09010400. The simulations were run in Shanghai Supercomputer Center. Part of the computing were carried on the SHAO Super Computing Platform. We acknowledge support from the MPG-CAS through the partnership programme between the MPIA group lead by A. Macciò and the PMO group lead by X. Kang

REFERENCES

- Allgood, B., Flores, R. A., Primack, J. R., et al. 2006, MNRAS, 367, 1781
- Agustsson, I., & Brainerd, T. G. 2006, ApJ, 650, 550
- Agustsson, I., & Brainerd, T. G. 2010, ApJ, 709, 1321
- Angulo, R. E., Lacey, C. G., Baugh, C. M., & Frenk, C. S. 2009, MNRAS, 1254
- Azzaro, M., Patiri, S. G., Prada, F., & Zentner, A. R. 2007, MNRAS, 376, L43
- Bailin, J., & Steinmetz, M. 2004, ApJ, 616, 27
- Bailin, J., & Steinmetz, M. 2005, ApJ, 627, 647
- Bailin, J., Power, C., Norberg, P., Zaritsky, D., & Gibson, B., 2008, MNRAS, 390, 1133
- Basilakos, S., Plionis, M., Yepes, G., Gottlöber, S., & Turchaninov, V. 2006, MNRAS, 365, 539
- Bett, P., Eke, V., Frenk, C. S., Jenkins, A., & Okamoto, T. 2010, MNRAS, 404, 1137
- Brainerd, T. G. 2005, ApJ, 628, L101
- Chen, D. N., Jing, Y. P., & Yoshikaw, K. 2003, ApJ, 597, 35
- Croton, D. J., Springel, V., White, S. D. M., De L., G., et al., 2006, MNRAS, 365, 11
- Deason, A., McCarthy, I., Font, A., Evans, N., Frenk, C., Belokurov, V., Libeskind, N., Crain, R., & Theuns, T., 2011, MNRAS, 415, 2607
- De Lucia, G., Kauffmann, G., Springel, V., White, S. D. M., Lanzoni, B., Stoehr, F., Tormen, G., & Yoshida, N. 2004, MNRAS, 348, 333
- Diemand, J., Kuhlen, M., & Madau, P. 2008, ApJ, 679, 1680
- Er, X., & Schneider, P., 2011, *ã*, 528, 52
- Faltenbacher, A., & Gottlöber, S. 2002, *Tracing Cosmic Evolution with Galaxy Clusters*, 268, 359
- Faltenbacher, A., Allgood, B., Gottlöber, S., Yepes, G., & Hoffman, Y. 2005, MNRAS, 362, 1099
- Faltenbacher, A., Li, C., Mao, S., van den Bosch, F. C., Yang, X., Jing, Y. P., Pasquali, A., & Mo, H. J. 2007, ApJ, 662, L71
- Faltenbacher, A., Jing, Y. P., Li, C., et al. 2008, ApJ, 675, 146
- Faltenbacher, A., Li, C., White, S. D. M., Jing, Y.-P., Shu-DeMao, & Wang, J. 2009, *Research in Astronomy and Astrophysics*, 9, 41
- Gan, J.L., Kang X., van den Bosch, F.C., & Hou, J.L., 2010, MNRAS, 408, 2201
- Gao, L., De Lucia, G., White, S. D. M., Jenkins, A., 2004, MNRAS, 352, L1
- Gerhard, O. E. 1983, MNRAS, 202, 1159
- Guo, Q., White, S., Boylan-Kolchin, M., De Lucia, G., et al., 2011, MNRAS, 413, 101

- Hoekstra, H., Yee, H., Gladders, M., 2014, *ApJ*, 606, 67
- Holmberg, E. 1969, *Arkiv for Astronomi*, 5, 305
- Hopkins, P. F., Bahcall, N. A., & Bode, P. 2005, *ApJ*, 618, 1
- Ibata, R., Lewis, G. F., Irwin, M., Totten, E., & Quinn, T., 2001, *ApJ*, 551, 294
- Jing, Y. P., & Suto, Y. 2002, *ApJ*, 574, 538
- Jing, Y. P., Börner, G., & Suto, Y. 2002, *ApJ*, 564, 15
- Jing, Y. P., Zhang P. J., Lin W. P., Gao L., & Springel V., 2006, *ApJ*, 640, L119
- Kang, X., Mao, S., Gao, L., & Jing, Y.P., 2005, *ã*, 437, 383
- Kang, X., van den Bosch, F. C., Yang, X., Mao, S., Mo, H. J., Li, C., & Jing, Y. P. 2007, *MNRAS*, 378, 1531
- Kang, X., van den Bosch, F. C., 2008, *ApJ*, 676, 101
- Kasun, S. F., & Evrard, A. E. 2005, *ApJ*, 629, 781
- Kazantzidis, S., Kravtsov, A. V., Zentner, A. R., et al. 2004, *ApJ*, 611, L73
- Lacey, C., & Cole, S. 1993, *MNRAS*, 262, 627
- Lacey, C., & Cole, S. 1994, *MNRAS*, 271, 676
- Lee, J., Kang, X., & Jing, Y. P., 2005, *ApJ*, 629, L5
- Li, Cheng, Jing, Y.P., Faltenbacher, A., & Wang, Ji., 2013, *ApJ*, 770, L12
- Li, Z., Wang Y., Yang X., Chen X., et al., 2013, *ApJ*, 768, 20
- Libeskind, N. I., Frenk, C. S., Cole, S., et al. 2005, *MNRAS*, 363, 146
- Libeskind, N., Cole, S., Frenk C., Okamoto T., & Jenkins A., 2007, *MNRAS*, 374, 16
- Lin, W. P., Jing, Y. P., & Lin, L. 2003, *MNRAS*, 344, 1327
- Lin, W. P., Jing Y. P., Mao S., Gao L., & McCarthy I.G., 2006, *ApJ*, 651, 636
- Ludlow, A. D., Navarro, J. F., Springel, V., et al. 2009, *ApJ*, 692, 931
- Lux, H., Lake, J., Johnston, K., 2012, *MNRAS*, 424, 16
- Macciò, A., Moore, B., Stadel, J., Diemand, J., 2006, *MNRAS*, 366, 1529
- Macciò, A. V., Dutton, A. A., & van den Bosch, F. C. 2008, *MNRAS*, 391, 1940
- Okumura, T., & Jing, Y. P. 2009, *ApJ*, 694, L83
- Okumura, T., Jing, Y. P., & Li, C. 2009, *ApJ*, 694, 214
- Olling, R.P., & Merrifield, M., 2000, *MNRAS*, 311, 361
- Porciani, C., Dekel, A., & Hoffman, Y. 2002, *MNRAS*, 332, 339
- Press, W. H., & Schechter, P. 1974, *ApJ*, 187, 425
- Springel, V., Yoshida, N., & White, S. D. M. 2001, *New A*, 6, 79
- Springel, V., White, S. D. M., Tormen G., & Kauffmann G. 2001, *MNRAS*, 328, 726
- Springel, V. 2005, *MNRAS*, 364, 1105
- Taylor, J.E., Babul A., 2001, *ApJ*, 559, 716
- van den Bosch, F. C., Abel, T., Croft, R. A. C., Hernquist, L., & White, S. D. M. 2002, *ApJ*, 576, 21
- Vera-Ciro, Carlos, Helmi, Amina, 2013, *ApJ*, 773, 4
- Vogelsberger, M., Genel, S., Sijacki, D., Torrey, P., Springel, V., Hernquist, L., 2013, *arXiv.1305.2913*
- Wang, H. Y., Jing, Y. P., Mao, S., & Kang, X. 2005, *MNRAS*, 364, 424
- Wang, H. Y., Mo, H. J., & Jing, Y. P. 2007, *MNRAS*, 375, 633
- Wang, Y., Yang, X., Mo, H. J., et al. 2008, *MNRAS*, 385, 1511
- Wang, Y., Park, C., Hwang, H. S., & Chen, X. 2010, *ApJ*, 718, 762
- White S.D.M., & Frenk C. S., 1991, *ApJ*, 379, 52
- White, S.D.M., & Rees, M. 1978, *MNRAS*, 183, 341
- Yang, X., van den Bosch, F. C., Mo, H. J., Mao, S., Kang, X., Weinmann, S. M., Guo, Y., & Jing, Y. P. 2006, *MNRAS*, 369, 1293
- Yang, X., Mo, H., van den Bosch, F., Zhang, Y., Han, J., 2012, *ApJ*, 752, 41
- Yang, X., Mo, H. J., Zhang, Y., & van den Bosch, F. C. 2011, *ApJ*, 741, 13
- Zentner, A. R., Berlind, A. A., Bullock, J. S., Kravtsov, A. V., & Wechsler, R. H. 2005, *ApJ*, 624, 505
- Zhu G., Zheng Z., Lin W. P., Jing Y. P., Kang X., & Gao L., 2006, *ApJ*, 639, L5